

Conjugated Poly(fluorene-quinoxaline) for Fluorescence Imaging and Chemical Detection of Nerve Agents with Its Paper-Based Strip

Seonyoung Jo,[†] Daigeun Kim,[†] Sang-Ho Son,[‡] Yongkyun Kim,[†] and Taek Seung Lee^{*,†,‡}

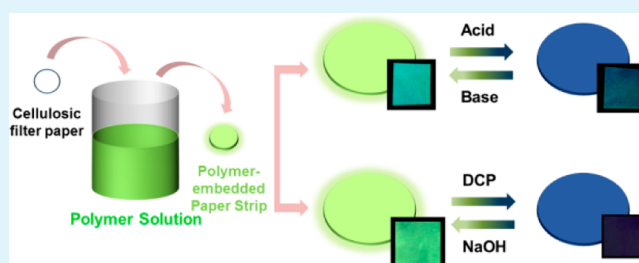
[†]Organic and Optoelectronic Materials Laboratory, Department of Advanced Organic Materials and Textile System Engineering, Chungnam National University, Daejeon 305-764, Korea

[‡]Organic and Optoelectronic Materials Laboratory, Graduate School of Green Energy Technology, Chungnam National University, Daejeon 305-764, Korea

S Supporting Information

ABSTRACT: Conjugated polymer of poly(fluorene-co-quinoxaline) was synthesized via Suzuki coupling polymerization. The emission color of the polymer can be tuned depending on the concentration of the polymer in solution. A low-energy bandgap is observed both in the concentrated solution and in the solid state, caused by aggregation of the polymer chains, resulting in long wavelength emission from the quinoxaline moiety, while short wavelength emission can be seen in diluted, well-dissolved solution. The presence of quinoxaline units enables us to demonstrate fluorescence switching and imaging. Paper-based strips containing the polymer are prepared via simple immersion of filter paper in the polymer solution for practical use in the detection of nerve agents. The emission of the paper-based strip is quenched upon exposure to diethyl chlorophosphate (DCP), a nerve agent simulant, and the initial emission intensity can be almost restored by treatment with aqueous sodium hydroxide solution, making a possible reversible paper-based sensor.

KEYWORDS: conjugated polymers, sensors, fluorescence, polyquinoxaline, nerve agents



INTRODUCTION

Fluorescent conjugated polymers have attracted much attention for their potential applications in organic light-emitting diodes, organic semiconductors, and chemical or biological sensors.^{1–5} The delocalized electronic structures of the conjugated polymers offer electronic coupling, which arises from intra- and intermolecular energy transfer.^{6,7} In particular, conjugated polymers have important features that bring about change in conductivity,^{8,9} exciton migration,^{10–14} and absorption or emission intensity,^{15,16} under external stimuli, resulting in substantial changes in measurable signals. Among them, chromogenic and fluorogenic sensors based on conjugated polymers have attracted attention in biological system, detection of chemicals, and environmental monitoring.^{17–19} Among the conjugated polymers, conjugated polyelectrolytes have been recognized as a promising platform for biosensing assay of biomolecules, ascribing to the water-solubility and favorable interaction with biomolecules.^{16,20–23}

One of the effective methods for developing perturbation of electronic structures of conjugated polymers leading to emission changes is related to the formation of a polymer aggregation or polymer complex upon exposure to external stimuli. The working mechanism is on the basis of the more efficient intermolecular energy transfer in the polymer aggregation state than in isolated polymer chains, such as in polymers in dilute solution.^{12,23} In a highly dissolved polymer solution of low concentration, exciton migration (energy

transfer) brings about within an isolated polymer chain. On the while, in a solution of high concentration or in the solid state, the polymer backbones are very close in distance, which enables excitons to migrate intermolecularly.¹⁵ As a result of intermolecular energy transfer in the aggregated polymers, blue-to-green or blue-to-red emission changes of conjugated polymers have been observed. This was subsequently used for the detection of biologically relevant species.^{20–26} On the basis of this mechanism, our group reported the synthesis of anionically charged conjugated polyelectrolytes composed of larger amounts of electron-donating phenylene units and relatively smaller amounts of electron-accepting benzothiadiazole or bithienylbenzothiadiazole segments to facilitate blue-to-green or blue-to-red emission color assays for mercury ions, proteins, and amino acids.^{14,27–29}

As one of the most popular classes of conjugated polymer units, a quinoxaline is known to be a typical electron-accepting group because of the strong electronegativity of the two nitrogen atoms. Many conjugated polymers with an electron donor–acceptor main chain have been prepared using quinoxaline or its derivatives as electron-withdrawing building blocks in their main chains.^{30–33}

Received: November 28, 2013

Accepted: December 30, 2013

Published: December 30, 2013

Nerve agents such as Sarin, Soman, and Tabun are known to be highly reactive, volatile, and lethal organophosphorous compounds, which disrupt the process by which nerves transfer messages to organs. The inhalation of nerve agents can lead to organ failure and eventual death within minutes.^{34,35} Therefore, a variety of detection methods for nerve agents have been developed; they are based on mass spectrometry, enzyme sensors, colorimetric probes, and fluorometric methods.^{36–48} Among them, fluorescence-based detection methods are known to be the simplest and most convenient for such applications because they do not require heavy instrumentation and they show changes in fluorescence that can be realized by naked-eye detection. It has been reported that functional groups such as alcohols, amines, and pyridines can react with organophosphorous derivatives via nucleophilic attack on phosphorous atoms in organophosphates.^{48,49}

In this study, we report a synthesis of partially π -electron-deficient polymer containing quinoxaline groups, **PQ**. Due to the presence of quinoxaline units linked with electron-donating fluorene groups, the polymer showed special features of concentration-dependent emission color change. Taking into account of this property, fluorescence imaging can be fabricated in the polymer films with the aid of a photoacid generator (PAG) and fluorescence switching can be accomplished by acid/base treatment. This polymer could be new type of sensor for the selective detection of a nerve agent simulant, such as diethyl chlorophosphate (DCP), in the form of a paper strip. Specific interaction between quinoxaline groups and nerve agents is expected via nucleophilic attack of quinoxalines to the electrophilic target, leading to fluorescence change. The solid-state sensing enables us to attain infield practical applications. It is known that the advantages of solid sensors over solution ones are related to the possibility of recycling, easier handling, and easier incorporation into devices.^{50–52} To the best of our knowledge, this is the first report on the synthesis of fluorescent polymer, the emission colors of which vary depending on the concentration, using quinoxaline units as an electron-accepting moiety instead of well-known benzothiadiazole groups, and subsequent applications in fluorescence imaging, switching, and sensing in a paper-based strip.

■ EXPERIMENTAL SECTION

Materials. Monomers and catalyst of Suzuki polymerization, such as 2,1,3-benzothiadiazole, 9,9-dioctylfluorene-2,7-diboronic acid bis-(1,3-propanediol) ester, 9,9-dioctyl-2,7-dibromofluorene, and tetrakis-(triphenylphosphine) palladium were purchased from Aldrich and used as received. Trifluoroacetic acid (TFA), triethylamine (TEA), and triphenylsulfonium triflate, as a PAG, were purchased from Aldrich and used as received. Organophosphorous compounds, including DCP, dimethyl methylphosphonate (DMMP), triethylphosphate (TEP), and tributylphosphate (TBP) were purchased from Aldrich and used without further purification. The chemical structures of the compounds are illustrated in Scheme S1 in the Supporting Information. Other chemicals were purchased from Samchun, Korea.

Characterization. The ¹H NMR and ¹³C NMR spectra were recorded on a Bruker DRX-300 spectrometer with tetramethylsilane as an internal standard (Korea Basic Science Institute). UV-vis absorption spectra were recorded on a PerkinElmer Lambda 35 spectrometer. Photoluminescence spectra were obtained from a Varian Cary Eclipse fluorescence spectrophotometer equipped with a xenon flash lamp excitation source. Elemental analysis was performed on an Elemental Analyzer EA 1108 (Fisons Instruments).

Synthesis of 5,8-Dibromoquinoxaline. 1,2-Diamino-3,6-diaminobenzene (0.93 g, 3.5 mmol), which was reduced from 4,7-dibromo-2,1,3-benzothiadiazole, was dissolved in acetic acid (30 mL).

Oxalaldehyde (0.693 g, 11.94 mmol) was added to the solution. The reaction mixture was refluxed for 18 h. On completion of the reaction, the mixture was precipitated in ethanol, isolated by filtration, and finally washed with ethanol. A greenish-yellow solid was collected (yield 0.8 g, 70%). The crude product was used without purification for the next reaction. ¹H NMR (300 MHz, CDCl₃): δ = 9.01 (d, 2H), 8.00 ppm (d, 2H). Anal. Calcd for C₈H₄Br₂N₂: C, 33.37; H, 1.40; N, 9.73. Found: C, 33.78; H, 1.31; N, 9.20.

Synthesis of 5,8-Dibromo-2,3-diphenylquinoxaline. 1,2-Diamino-3,6-dibromobenzene (0.8 g, 3 mmol) was dissolved in acetic acid (30 mL) and benzil (0.63 g, 3 mmol) was added, portion-wise, to the solution. After reflux for 18 h, the reaction mixture was precipitated in ethanol, isolated by filtration, and recrystallized from ethanol. Further purification was carried out by column chromatography with ethyl acetate and n-hexane (5 : 5, v/v). The product was dried in vacuo, affording a yellow solid (yield 0.5 g, 37 %). ¹H NMR (300 MHz, CDCl₃): δ = 7.73 (d, 2H), 7.66–7.64 (d, 4H), 7.57–7.54 ppm (m, 6H). Anal. Calcd for C₂₀H₁₂Br₂N₂: C, 54.58; H, 2.75; N, 6.36. Found: C, 54.74; H, 2.73; N, 6.47.

Synthesis of PQ. A round-bottomed flask was charged with 5,8-dibromoquinoxaline (0.02 g, 0.069 mmol), 9,9-dioctyl-2,7-dibromofluorene (0.34 g, 0.621 mmol), and 9,9-dioctyl fluorene-2,7-diboronic acid bis-(1,3-propanediol) ester (0.492 g, 0.828 mmol), and then purged with nitrogen gas. The flask was degassed several times to ensure the complete removal of oxygen. After degassing, toluene (5 mL), Pd(PPh₃)₄ (0.047 g, 0.041 mmol), 2 M aqueous potassium carbonate solution (3 mL), and water (2 mL) were added to the reaction mixture. The mixture was refluxed for 48 h. After cooling, the mixture was poured into excess methanol and the precipitate was washed with acetone, methanol, and water, affording a green powder (yield 0.40 g, 77 %). ¹H NMR (300 MHz, CDCl₃): δ = 7.87–7.69 (m), 2.13 (t), 1.28–0.80 ppm (m). ¹³C NMR (CDCl₃): δ = 121.51, 55.35, 40.37, 31.80, 30.93, 30.04, 29.23, 23.91, 22.60, 14.07 ppm. FT-IR (cm⁻¹): 2925 (sp³ C–H), 1608 (C=N), 1458 (aryl C=C). Anal. Calcd for C_{55.3}H_{77.3}N_{0.26}: C, 89.1; H, 10.5; N, 0.50. Found: C, 88.2; H, 9.85; N, 0.49.

Fluorescence Patterning. A thin film of **PQ** formulated with triphenylsulfonium triflate (1 wt % with respect to **PQ**) as a PAG was obtained via spin-casting from a 1 wt % chloroform solution on a silicon wafer. The film was exposed through a photomask with a monochromic 254 nm hand held UV lamp (intensity of 630 μ W/cm²) for 10 min. The fluorescence images were recorded using an Olympus BX53 fluorescence microscope.

Preparation of Paper-Based Strip. A cellulosic filter paper (Advantec No. 2) with a diameter of 5 mm was immersed in a chloroform solution of **PQ** (1.0 \times 10⁻⁵ M) and then air-dried. The test strips were prepared to use for assessing acid-base switching behavior and for a detection of nerve agent.

Acid–Base Switching Test (Solution Test). TFA in chloroform solution (100 mM) was added to a chloroform solution of **PQ** (1.0 \times 10⁻⁴ M). The mixture was stirred for 1 min at room temperature. Subsequently, addition of TEA in chloroform (100 mM) was carried out similar to the case of TFA. At each step, the optical properties of the solutions were measured with absorption and fluorescence spectrometers.

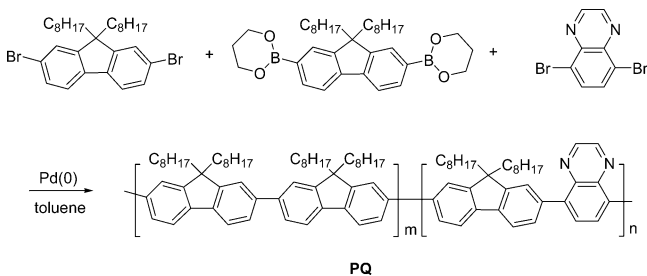
Acid–Base Switching Test (Strip Test). A paper strip containing **PQ** was exposed to acidic gas from hydrochloric acid and basic vapor of TEA vapor, consecutively, in a closed chamber, as shown in Figure S3b in the Supporting Information. Acidic gas or basic vapors were generated by keeping the filter paper strip for <5 min in a closed vial under ambient condition. The fluorescence spectra were recorded for each cycle.

Nerve Agent Simulant Detection. Nerve gas detection was carried out with **PQ** paper strips. Strips were immersed in the different organophosphorous compounds (DCP, DMMP, TEP and TBP) in concentrations ranging from 6.0 \times 10⁻⁴ M to 1.8 \times 10⁻³ M in ethanol solution for 1 min and then air-dried. Variation in the fluorescence spectra of the strips in the presence and absence of nerve gas simulants were recorded.

RESULTS AND DISCUSSION

The quinoxaline monomers 5,8-dibromoquinoxaline was synthesized by a reaction of 1,2-diamino-4,7-dibromobenzene with oxalaldehyde, respectively, according to previously published methods.^{31,53} The compound 1,2-diamino-4,7-dibromobenzene was prepared by a reduction of 4,7-dibromo-2,1,3-benzothiadiazole in the presence of sodium borohydride. For the preparation of poly(flourene-co-quinoxaline), **PQ**, conventional Suzuki cross-coupling polymerization was carried out in the presence of palladium catalyst, as shown in Scheme 1. The yields of **PQ** was 77%.

Scheme 1. Synthesis of **PQ**



The chemical structures of the polymer was determined by means of ¹H NMR, ¹³C NMR, FT-IR, and elemental analysis. To attain an efficient intermolecular exciton migration effect, the molar composition in the polymer is the primary concern. The molar composition (*m:n*) was found to be 0.87:0.13, determined by elemental analysis. The polymer comprised a larger amount of fluorene segments (as electron donor) and smaller amount of quinoxaline units (as electron acceptor). The donor–acceptor system is necessary to obtain completely different emissions between the solution state (from fluorene emission) and the solid state (from quinoxaline emission) via intramolecular and intermolecular energy transfer (exciton migration), respectively. To realize effective intermolecular energy transfer, the molar composition in the polymer should be carefully controlled. The molar compositions of above values were employed because only green emission was observed when the value of *n* exceeded 25 mol %, even in highly diluted solution.

The polymer was readily soluble in common organic solvents, including chloroform and THF. Molecular weight of the polymer were determined by gel permeation chromatography with polystyrene as a standard and chloroform as an eluent. The number average molecular weight (*M_n*) of **PQ** was found to be 6470 and weight average molecular weight (*M_w*) to be 15000 with polydispersity (PDI) of 2.32.

The UV-vis absorption and fluorescence spectra of **PQ** were recorded in chloroform at concentrations ranging from 1×10^{-6} to 1×10^{-4} M and in spin-cast thin films as shown in Figure 1. The maximum absorption wavelength of **PQ** in chloroform solution was 380 nm, which did not vary according to the concentrations of polymer. In contrast, the emission of the polymer was found to be highly concentration dependent. In dilute solutions of **PQ** (1.0×10^{-7} M), the emission spectra of polymers exhibited a strong blue emission at 416 nm from fluorene units, along with a shoulder at 440 nm and a weak emission band at 520 nm. The fluorescence spectra clearly indicate that the intrachain energy transfer (exciton migration) plays an important role in exhibiting the short-wavelength

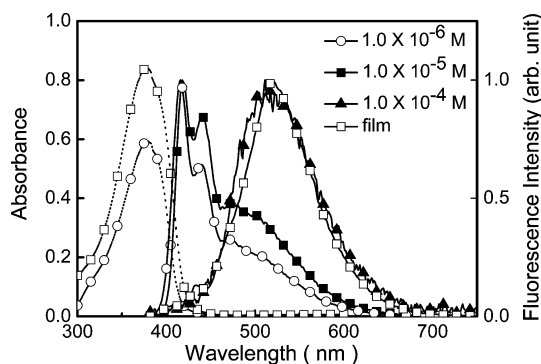


Figure 1. Absorption (dotted) and normalized fluorescence spectra (solid) of **PQ** in chloroform solution and in the film. For absorption spectra, \circ corresponds to the solution (1.0×10^{-5} M) and \square to the film.

emission (416 nm) originating from fluorene units, which are present in relatively large amounts in the backbone. As the concentration of **PQ** increases, the intensity of the blue emission gradually decreases. When the polymer concentration is further increased to 1.0×10^{-4} M, or in the film state, the emission spectra of **PQ** only exhibit green emission at 521 nm, originating from the quinoxaline units, in which interchain aggregation is induced with increasing local concentration of the fluorene units around the quinoxaline moiety, resulting in enhanced interchain energy transfer to quinoxaline.⁵⁴ The fluorescence changes of **PQ** upon concentration changes can be easily seen with the naked eye under illumination with a UV lamp (Figure 2).

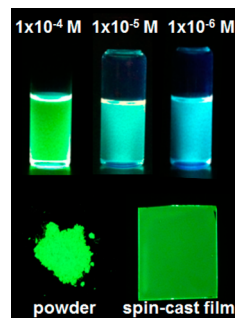
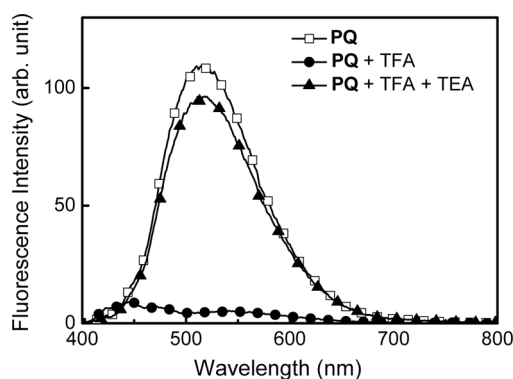


Figure 2. Fluorescence images of **PQ** in chloroform solutions and in the solids. Photographs were taken under UV irradiation (365 nm).

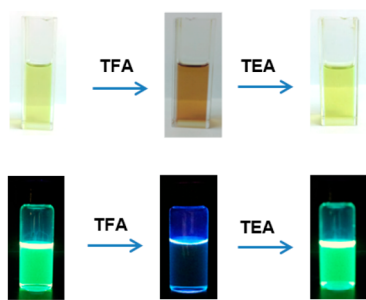
As **PQ** has basic quinoxaline segments in the backbones, molecular switching behavior is observed upon consecutive exposure to acid and base. The pale-yellow color of **PQ** in chloroform solution became dark brown upon addition of TFA; it exhibited a very small hyperchromic shift of absorption at 380 nm (see Figure S2a in the Supporting Information). Contrary to the negligible absorption color change in the presence of acid, the green fluorescence of **PQ** solution at 510 nm was completely quenched upon addition of TFA, with blue-shifted emission to 443 nm (see Figure S2b in the Supporting Information). The protonation of nitrogens in quinoxaline moieties resulted in retarded or forbidden intermolecular electron transfer from fluorene to quinoxaline. As a result, the emission at 510 nm (from quinoxaline units) decreased, whereas a small emission at 443 nm (fluorene segments) was maintained. The specified emission, i.e., short wavelength emission from fluorene units and long wavelength emission for

quinoxaline moiety, can be clearly seen in Figure S2c in the Supporting Information, which demonstrates quenching in long wavelength emission from quinoxaline moiety was observed upon protonation, indicating that the protonation influenced the electron density of the quinoxaline units, not the density of the fluorene moieties.

As shown by the spectral changes and in photographs in Figure 3, the initial green fluorescence of PQ (1.0×10^{-4} M)



(a)



(b)

Figure 3. (a) Spectral changes and (b) alteration in ambient colors and emission colors of PQ (1.0×10^{-4} M) upon consecutive addition of TFA and TEA (100 equiv each) in chloroform solution.

can be almost restored ($\sim 90\%$) upon addition of the base TEA which acted as a proton scavenger.³¹ Besides such a switching behavior in solution, the reversible fluorescence switching behavior of PQ-embedded cellulosic filter paper in the presence of acidic gas (from HCl) and basic vapor (from TEA) was easily obtained. Figure S3 in the Supporting Information demonstrates fluorescence switching of PQ adsorbed on cellulosic filter paper upon consecutive exposure to acidic gas and basic vapor. In the presence of acidic gas, the bluish-green fluorescence was readily quenched and changed to dark-blue fluorescence, mainly because of the protonation of nitrogen in quinoxaline. Upon exposure to basic vapor, the bluish-green fluorescence of PQ was recovered by deprotonation. The pH responsiveness of fluorescence in PQ showed a reversible fashion in the presence of the acid–base during several cycles.

As mentioned above, PQ showed fluorescence change upon addition of acid because of the presence of quinoxaline units. This can be used in fluorescence patterning by simple UV irradiation without subsequent baking or etching, which is frequently employed for patterning.^{55–58} The latent fluorescent images were constructed on a spin-cast film of PQ in the presence of PAG through a photomask by illumination of a hand-held UV lamp (254 nm) for 10 min. The bright-green

fluorescent image could be fabricated on the unexposed area through the photomask. A micropattern with line width $2 \mu\text{m}$ was successfully constructed, as shown in Figure 4. Because the

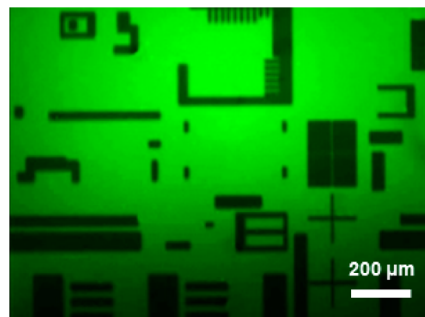


Figure 4. Fluorescence patterned images of spin-cast film of PQ through a photomask on a silicon wafer. Fluorescence images were fabricated under UV irradiation (254 nm) with a hand-held UV lamp for 10 min ($630 \mu\text{W}/\text{cm}^2$). Green fluorescent area was unexposed to UV.

patterns were fabricated as latent images, they could not be seen under ambient light, whereas highly fluorescent patterns were clearly observed under UV illumination.

Finally, we demonstrated a nerve agent sensor for DCP, which is a nerve agent mimic. For the practical application of a sensor of PQ, paper-based strips were prepared by simple immersion of a small piece of cellulosic filter paper in a chloroform solution of PQ (1×10^{-5} M) and then dried in air. The PQ-embedded paper strips also exhibited a specific emission color, which is highly dependent on the concentration of PQ (see Figure S4 in the Supporting Information). The sensor strip was immersed in a solution containing organophosphorous compounds for 10 min at ambient temperature, whereafter an emission change of the sensor strip was observed. The quinoxaline groups in the polymer backbone should interact with the phosphorous atom in DCP. Then, as a result, emission quenching or shift of the PQ strip is expected upon exposure to the organophosphorous compound DCP. The PQ strip was stable in ethanol solution, which was a medium for DCP sensing, for 90 min, indicating that the PQ is stable to bleaching in solution (see Figure S5 in the Supporting Information).

The fluorescence response of a PQ paper strip to DCP in the concentration range of 0 to 0.01 M is shown in Figure 5a. There is gradual emission quenching with an increasing concentrations of DCP. To further investigate the quantitative relationship between the emission of a PQ strip and the concentration of DCP, the quenching response was observed through measurement of the Stern–Volmer constant (K_{SV}), described by the equation ($I_0/I = 1 + K_{SV}[Q]$), where I_0 and I are the fluorescence intensities without DCP and with DCP, respectively, K_{SV} corresponds to the Stern–Volmer constant, and Q means the quencher (DCP) (Figure 5b).⁵ The K_{SV} of the PQ strip was calculated from the slope and found to be 329 M^{-1} . The limit of detection (LOD) of the PQ paper strip was found to be 1.49×10^{-5} M (based on the $3\sigma/\text{slope}$, where σ is the standard deviation of four independent measurements).⁵⁹

To obtain some insight into the selective detection of DCP with a PQ strip, we carried out parallel experiments in ethanol with DMMP, TEP, and TBP, which are organophosphorous compounds with structures similar to DCP. The spectroscopic changes shown in Figure 6 reveal that the PQ strip did not

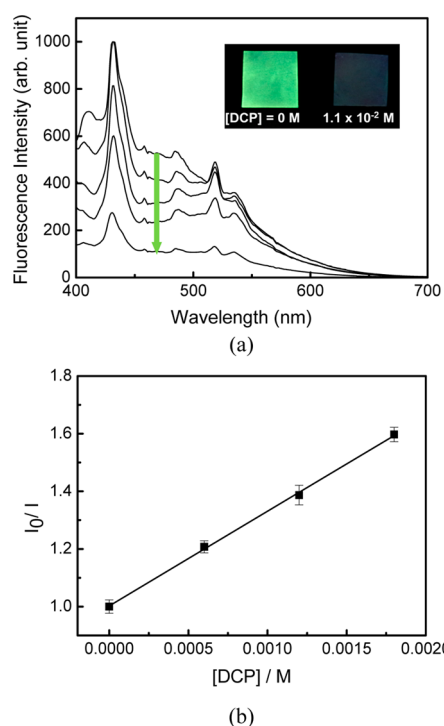


Figure 5. (a) Changes in fluorescence spectra of the PQ-embedded paper strip (1×10^{-5} M) with different concentrations of DCP (from top to bottom, $[\text{DCP}] = 0$; 1.0×10^{-4} ; 1.1×10^{-3} ; 1.1×10^{-2} ; 1.1×10^{-1} M. Inset photo represents emission quenching of PQ strip upon exposure to DCP. (b) Stern–Volmer plot of the PQ strip in response to DCP. I_0 and I correspond to emission intensity at 433 nm in the absence and presence of DCP, respectively.

show any significant changes in emission upon exposure to DMMP, TEP, and TBP. For the purpose of comparison, the relative fluorescence intensity (I_0/I) of the PQ strip was measured after the addition of DMMP, TEP, TBP, and DCP in the concentration range of 0 to 18 mM. The PQ strip showed high selectivity toward DCP (Figure 7). The K_{SV} values calculated for DMMP (70 M^{-1}), TEP (19 M^{-1}), and TBP (3 M^{-1}) are much lower than the value for DCP (329 M^{-1}). The high selectivity of PQ strip toward DCP is attributed to the difference in electrophilicity of organophosphorous compounds. The sensing mechanism is based on the nucleophilic attack of quinoxaline group to organophosphorous compounds and, thereby, PQ attacks to electron-deficient DCP more easily than other compounds.

The quenched fluorescence of a PQ strip upon addition of DCP was almost recovered when the strip was treated with aqueous sodium hydroxide solution. As this process is reversible, the result implies that the strip sensor based on PQ allows us to apply it to a movable, portable, reversible sensor for the detection of DCP in environmental fields (see Figure S6 in the Supporting Information).

As illustrated in Scheme 2, the PQ-embedded paper strip exhibited not only fluorescence switching behavior under acid/base atmosphere but also fluorescence quenching behavior in the presence of DCP.

CONCLUSIONS

We synthesized poly(fluorene-co-quinoxaline), which has dominant fluorene units in the backbone. The polymer has characteristic features of emission color tuning based upon its

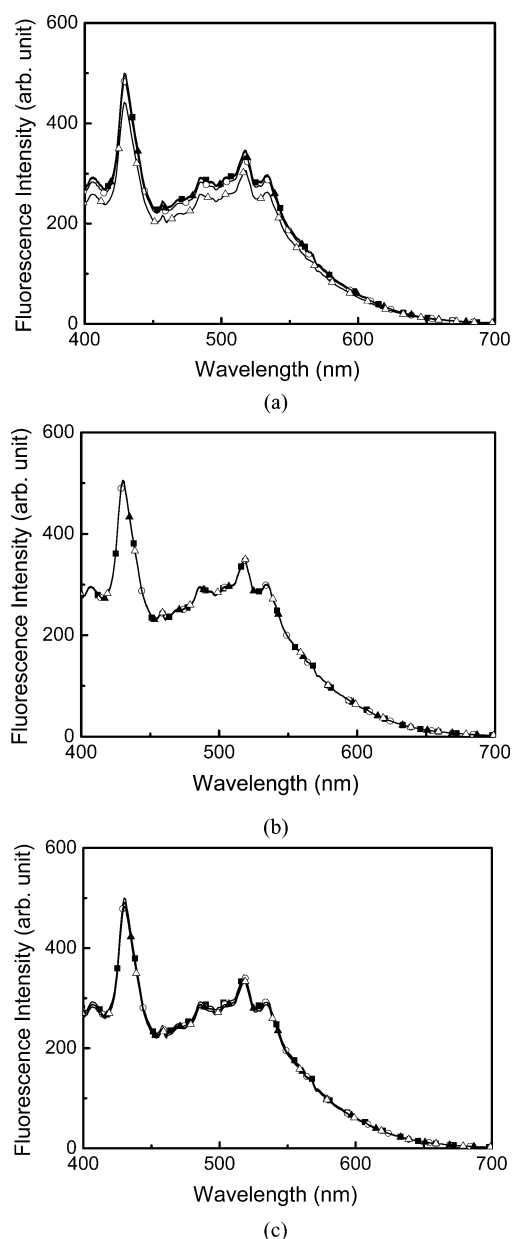


Figure 6. Changes in fluorescence spectra of the PQ-embedded strip (1.0×10^{-5} M) upon addition of (a) DMMP, (b) TBP, and (c) TEP at different concentration (\blacksquare , 0 M; \circ , 6.0×10^{-4} M; \blacktriangle , 3.2×10^{-3} M; \blacktriangledown , 1.8×10^{-2} M) in ethanol.

phases such as solution and solid, caused by intramolecular and intermolecular aggregation, respectively. In the solid state, interchain exciton migration to a low-energy quinoxaline moiety is facilitated and, thereby, emission at long wavelength (corresponding to quinoxaline) is exhibited. Because of the presence of the basic quinoxaline moiety in the polymer, fluorescence switching by acid/base and fluorescence patterning could be realized effectively in solution and in a film, respectively. The highly sensitive and selective detection of a nerve agent mimic was accomplished in the form of a solid paper strip containing the polymer. The change in fluorescence was clearly observed by the naked eye. The LOD of the paper strip was found to be $\sim 1.49 \times 10^{-5}$ M. This value is rather low compared to what is reported in other studies.^{46,60} This system

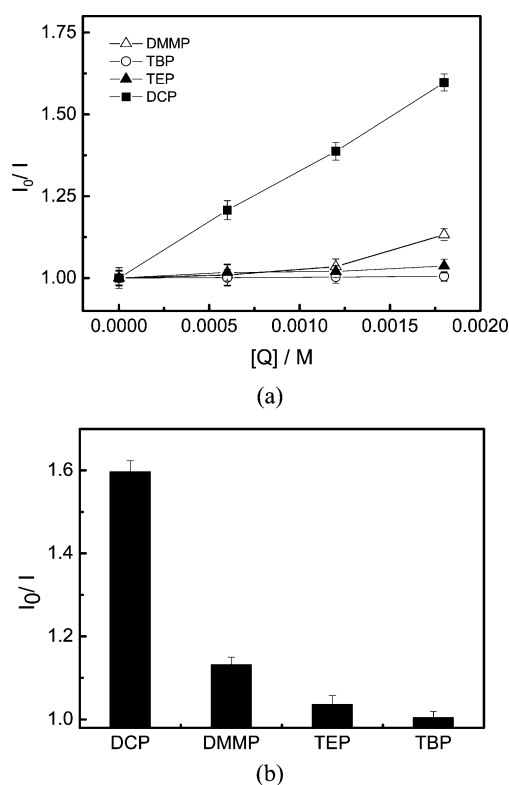
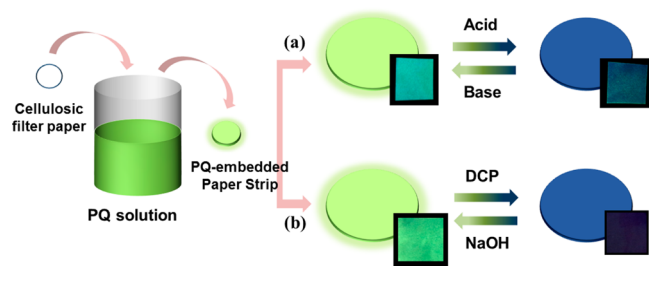


Figure 7. (a) Comparison of Stern–Volmer plots of the PQ strips in response to DCP (■), DMMP (Δ), TBP (○), and TEP (▲). (b) Relative fluorescence intensity of the PQ strips by addition of organophosphorous compounds. I_0 and I correspond to emission intensity at 433 nm in the absence and presence of organophosphorous compounds, respectively.

Scheme 2. Schematic Illustration of (a) Acid–Base Switching and (b) DCP Sensing with Paper-Based PQ Strip; Inset Photos Were Taken under UV Irradiation (365 nm)



can be useful for the turn-off detection of nerve agents in terms of portability, ease of handling, and cost effectiveness.

■ ASSOCIATED CONTENT

Supporting Information

Chemical structures of nerve agents, absorption and fluorescence spectra of the polymer in THF, and switching data. This material is available free of charge via the Internet at <http://pubs.acs.org>.

■ AUTHOR INFORMATION

Corresponding Author

*E-mail: tslee@cnu.ac.kr. Phone: +82-42-821-6615. Web site: <http://www.onom.re.kr>.

Notes

The authors declare no competing financial interest.

■ ACKNOWLEDGMENTS

This research was supported by Basic Science Research Program (2012R1A2A2A01004979) through the National Research Foundation of Korea (NRF) funded by Korean government.

■ REFERENCES

- (1) Burroughes, J. H.; Brandly, D. D. C.; Brown, A. R.; Marks, R. N.; Mackay, K.; Friend, R. H.; Burns, P. L.; Holmes, A. B. *Nature* **1990**, *347*, 539–541.
- (2) Mozer, A. J.; Denk, P.; Scharber, M. C.; Neugebauer, H.; Sariciftci, N. S.; Wangner, P.; Lusten, L.; Vanderzande, D. *J. Phys. Chem. B* **2004**, *108*, 5235–5242.
- (3) Heeger, A. J. *Chem. Soc. Rev.* **2010**, *39*, 2354–2371.
- (4) Campbell, I. H.; Smith, D. L. *Physics of Polymer Light-Emitting Diodes*. In *Semiconducting Polymers*; Hadziioannou, G., van Hutten, P. F., Eds.; Wiley-VCH: Weinheim, Germany, 2000; pp 333–364.
- (5) Thomas, S. W., III; Joly, G. D.; Swager, T. M. *Chem. Rev.* **2007**, *107*, 1339–1386.
- (6) Weber, S. E. *Chem. Rev.* **1990**, *90*, 1469–1482.
- (7) Guillet, J. E. *Polymer Photophysics and Photochemistry*; Cambridge University Press: Cambridge, U.K., 1985.
- (8) Garnier, F.; Korri, Y. H.; Srivastava, P.; Mandrand, B.; Delair, T. *Synth. Met.* **1999**, *100*, 89–94.
- (9) Korri-Youssoufi, H.; Yassar, A. *Biomacromolecules* **2001**, *2*, 58–64.
- (10) Kim, Y.; Bouffard, J.; Kooi, S. E.; Swager, T. M. *J. Am. Chem. Soc.* **2005**, *127*, 13726–13731.
- (11) Kim, Y.; Whitten, J. E.; Swager, T. M. *J. Am. Chem. Soc.* **2005**, *127*, 12122–12130.
- (12) Satrijo, A.; Swager, T. M. *J. Am. Chem. Soc.* **2007**, *129*, 16020–16028.
- (13) Yu, D.; Zhang, Y.; Liu, B. *Macromolecules* **2008**, *41*, 4003–4011.
- (14) Lee, J. H.; Kim, D. G.; Kwon, N. Y.; Jang, G.; Son, J. H.; Lee, M. J.; Cho, H.; Kweon, H.; Lee, T. S. *J. Polym. Sci., Part A: Polym. Chem.* **2011**, *49*, 138–146.
- (15) Kumaraswamy, S.; Bergstedt, T.; Shi, X.; Rininsland, F.; Kushon, S.; Xia, W. S.; Ley, K.; Achyuthan, K.; McBranch, D.; Whitten, D. G. *Proc. Natl. Acad. U.S.A.* **2004**, *101*, 7511–7515.
- (16) Pinto, M. R.; Schanze, K. S. *Proc. Natl. Acad. U.S.A.* **2004**, *101*, 7505–7510.
- (17) McQuade, D. T.; Pullen, A. E.; Swager, T. M. *Chem. Rev.* **2000**, *100*, 2537–2574.
- (18) McQuade, D. T.; Hegedus, A. H.; Swager, T. M. *J. Am. Chem. Soc.* **2000**, *122*, 12389–12390.
- (19) Swager, T. M. *Acc. Chem. Res.* **1998**, *31*, 201–207.
- (20) Liu, B.; Bazan, G. C. *J. Am. Chem. Soc.* **2004**, *126*, 1942–1943.
- (21) Pu, K. –Y.; Zhan, R.; Liu, B. *Chem. Commun.* **2010**, *46*, 1470–1472.
- (22) Wang, Y.; Zhan, R.; Li, T.; Pu, K. –Y.; Wang, Y.; Tan, Y. C.; Liu, B. *Langmuir* **2012**, *28*, 889–895.
- (23) Satrijo, A. S.; Kooi, E.; Swager, T. M. *Macromolecules* **2007**, *40*, 8833–8841.
- (24) Ho, H. A.; Leclerc, M. *J. Am. Chem. Soc.* **2003**, *125*, 4412–4413.
- (25) Ho, H. A.; Leclerc, M. *J. Am. Chem. Soc.* **2004**, *126*, 1384–1387.
- (26) Zhang, T.; Fan, H. L.; Zhou, J. G.; Liu, G. L.; Feng, G. D.; Jin, Q. H. *Macromolecules* **2006**, *39*, 7839–7843.
- (27) Kwon, N. Y.; Kim, D. G.; Son, J. H.; Jang, G.; Lee, J. H.; Lee, T. S. *Macromol. Rapid Commun.* **2011**, *32*, 1061–1065.
- (28) Kwon, N. Y.; Jang, G.; Kim, D.; Kim, J.; Lee, T. S. *J. Polym. Sci., Part A: Polym. Chem.* **2013**, *51*, 2393–2400.
- (29) Kwon, N. Y.; Kim, D.; Jang, G.; Lee, J. H.; So, J. –H.; Kim, C. –H.; Kim, T. H.; Lee, T. S. *ACS Appl. Mater. Interfaces* **2012**, *4*, 1429–1433.
- (30) Inganäs, O.; Zhang, F.; Tvingstedt, K.; Andersson, L. M.; Hellström, S.; Andersson, M. R. *Adv. Mater.* **2010**, *22*, 100–116.

- (31) Kim, H. J.; Lee, J. H.; Lee, M.; Lee, T. S. *React. Funct. Polym.* **2008**, *68*, 1696–1703.
- (32) Duan, R.; Ye, L.; Guo, X.; Huang, Y.; Wang, P.; Zhang, S.; Zhang, J.; Huo, L.; Hou, J. *Macromolecules* **2012**, *45*, 3032–3038.
- (33) Du, X.; Qi, J.; Zhang, Z.; Ma, D.; Wang, Z. Y. *Chem. Mater.* **2012**, *24*, 2178–2185.
- (34) Marrs, T. C. *Pharmacol. Ther.* **1993**, *58*, 51–66.
- (35) Sidell, F. R.; Borak, J. *Ann. Emerg. Med.* **1992**, *21*, 865–871.
- (36) Gehauf, B.; Goldenson, J. *Anal. Chem.* **1957**, *29*, 276–278.
- (37) Kim, K.; Tsay, O. G.; Atwood, D. A.; Churchill, D. G. *Chem. Rev.* **2011**, *111*, 5345–5403.
- (38) Zhang, S. -W.; Swager, T. M. *J. Am. Chem. Soc.* **2003**, *125*, 3420–3421.
- (39) Dale, T. J.; Rebek, J., Jr. *J. Am. Chem. Soc.* **2006**, *128*, 4500–4501.
- (40) Ilhan, F.; Tyson, D. S.; Meador, M. A. *Chem. Mater.* **2004**, *16*, 2978–2980.
- (41) Wallace, K. J.; Fagbemi, R. I.; Folmer-Andersen, F. J.; Morey, J.; Lynch, V. M.; Anslyn, E. V. *Chem. Commun.* **2006**, 3886–3888.
- (42) Menzel, E. R.; Menzel, L. W.; Schwierking, J. R. *Talanta* **2005**, *67*, 383–387.
- (43) Wallace, K. J.; Morey, J.; Lynch, V. M.; Anslyn, E. V. *New J. Chem.* **2005**, *29*, 1469–1474.
- (44) Dale, T. J.; Rebek, J., Jr. *Angew. Chem. Int. Ed.* **2009**, *48*, 7850–7852.
- (45) Burnworth, M. S.; Rowan, J.; Weder, C. *Chem.—Eur. J.* **2007**, *13*, 7828–7836.
- (46) Wu, W.; Dong, J.; Wang, X.; Li, J.; Sui, S.; Chen, G.; Liu, J.; Zhang, M. *Analyst* **2012**, *137*, 3224–3226.
- (47) Kim, T. H.; Li, G.; Park, W. H.; Lee, T. S. *Mol. Cryst. Liq. Cryst.* **2006**, *445*, 185–190.
- (48) Lim, H. J.; Lee, J. H.; Lee, H.; Lee, J. H.; Lee, J. H.; Jung, J. H.; Kim, J. S. *Adv. Funct. Mater.* **2011**, *21*, 4035–4040.
- (49) Chulvi, K.; Gaviña, P.; Costero, A. M.; Gil, S.; Parra, M.; Gotor, R.; Royo, S.; Martínez-Máñez, R.; Sancenón, F.; Vivancos, J. *Chem. Commun.* **2012**, *48*, 10105–10107.
- (50) Gole, B.; Shanmugaraju, S.; Bar, A. K.; Mukherjee, P. S. *Chem. Commun.* **2011**, *47*, 10046–10048.
- (51) Rolland, J. P.; Mourey, D. A. *MRS Bull.* **2013**, *38*, 299–305.
- (52) Su, S.; Ali, M. M.; Filipe, C. D. M.; Li, Y.; Pelton, R. *Biomacromolecules* **2008**, *9*, 935–941.
- (53) Gunbas, G. E.; Durmus, A.; Toppare, L. *Adv. Mater.* **2008**, *20*, 691–695.
- (54) Le, V. S.; Kim, B.; Lee, W.; Jeong, J.; Yang, R.; Woo, H. Y. *Macromol. Rapid Commun.* **2013**, *34*, 772–778.
- (55) Palacios, M.; García, O.; Hernández, J. R. *Langmuir* **2013**, *29*, 2756–2763.
- (56) Huh, S.; Kim, S. B. *J. Phys. Chem. C.* **2010**, *114*, 2880–2885.
- (57) Lee, J.; Yarimaga, O.; Lee, C. H.; Choi, Y. -K.; Kim, J. -M. *Adv. Funct. Mater.* **2011**, *21*, 1032–1039.
- (58) Lee, J. K.; Kim, H. -J.; Kim, T. H.; Lee, C. -H.; Park, W. H.; Kim, J.; Lee, T. S. *Macromolecules* **2005**, *38*, 9427–9433.
- (59) Thomsen, V.; Schatzlein, D.; Mercurio, D. *Spectroscopy* **2003**, *18*, 112–114.
- (60) Royo, S.; Martínez-Máñez, R.; Sancenón, F.; Costero, A. M.; Parra, M.; Gil, S. *Chem. Commun.* **2007**, 4839–4847.